Chapter 3

Design of SLIM for electromagnetic launch under constant current excitation

3.1 Introduction

This Chapter deals with the design of SLIM for electromagnetic propulsion under constant current excitation. A mathematical model of the same is presented and an ideal case of launch using SLIM is discussed initially and later on the actual characteristics of the designed SLIM are used for establishing the relation between force and velocity. For analytical calculation of the steady-state thrust-velocity characteristics of a SLIM, Parseval's method of Fourier Transform [5] has been adopted.

3.2 Mathematical Model

For simplifying the modeling of the launch system, consider a body of mass m placed on a plane inclined at an angle θ with the horizontal Earth's surface. The electromagnetic force F (thrust) generated by the SLIM along the inclined plane is continuously applied to the

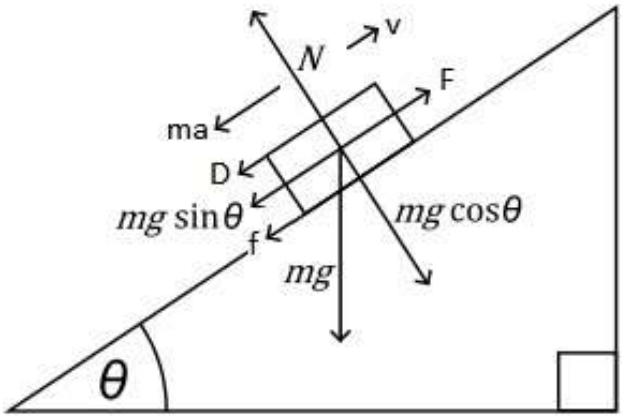

Fig. 3.1 Simplified model of the EM launch system

body (mover secondary of the SLIM and the payload attached to it) and it moves with a velocity v. From Fig.3.1 the forces acting on the body are:

- The external force (electromagnetic Thrust generated by the SLIM), F
- The normal direction electromagnetic force generated by the SLIM, N
- A component of the weight of the mass opposite to the direction of motion, $mg\ sin\ \theta$
- Frictional force acting between the wheel and the rail, opposite to the direction of motion, f
- Drag force, the aerodynamic force opposing the body's motion through the air, D
- Pseudo-force, ma

Balancing these forces from the free body diagram gives the following equation:

$$F - ma = mg\ sin\theta + f + D \tag{3.1}$$

In (3.1), the following relations can be substituted:

$$a = \frac{dv}{dt} \tag{3.2}$$

$$f = \mu\ (mg\ cos\theta - N) \tag{3.3}$$

$$D = b\ v^2 \tag{3.4}$$

where μ is the coefficient of kinetic friction and b is the coefficient of drag force. Then the equation of motion becomes,

$$F - m\frac{dv}{dt} = mg\ sin\theta + \mu\ (mg\ cos\theta - N) + b\ v^2 \tag{3.5}$$

It will become evident in Section 3.3.3 from Fig. 3.14b, that the normal force generated by the designed SLIM is repulsive in the region of interest i.e. between standstill and a little beyond 50 m/s (exit velocity of the projectile). The secondary mover of the SLIM is considered to be placed above the primary stator. The generated normal force will levitate the mover which is controlled by friction to overcome the normal and lateral displacements. In EM launch applications, tremendous amount of electrical energy flows in the stator coils of the LIM for a short duration to provide maximum acceleration to the projectile. To avoid insulation breakdown in the coils due to the heat generated in them, the operating time of the launcher should be kept as low as possible, while achieving the desired performance. For this purpose, the characteristic between the applied force, which would be generated by the LIM stator, and the velocity must be as close to an inverse linear relationship as possible. By avoiding the positive slope region in the usual force-velocity characteristic of an LIM, the starting (accelerating) time of the motor reduces significantly. Another option is to provide a constant thrust by V/F method for launch application wherein the thrust requirement is almost half the value of peak thrust requirement in inverse linear characteristics. Though inverse linear characteristic results in quick launch. Thus, the

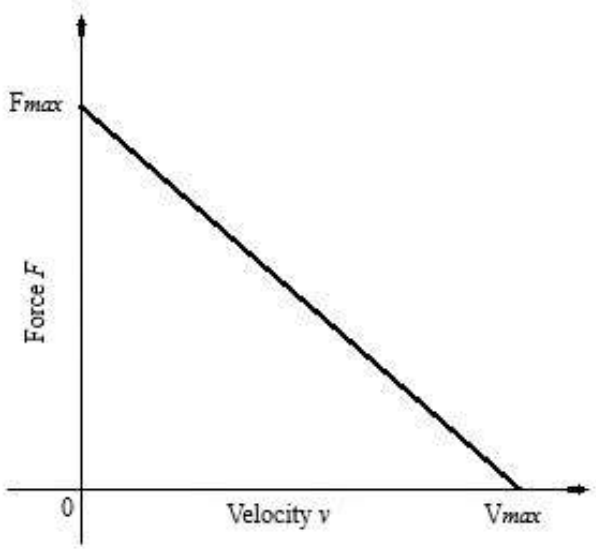

Fig. 3.2 Assumed inverse linear force-velocity characteristic of the LIM

following relation between the force F and the velocity v is assumed:

$$F = F_{max} - \frac{F_{max}}{v_{max}} v \tag{3.6}$$

where F_{max} *and* v_{max} are the maximum limit of force and velocity starting from 0 (Fig. 3.2).

Equations (3.5) and (3.6) describe the accelerated motion of the body up the inclined plane. These two equations were setup in MATLAB Simulink (Fig. 3.3). Also, a script was written in MATLAB to find the required value of starting force F_{max} to satisfy the launcher requirements.

SIMULATION AND RESULTS

The following parameters (Table 3.1) were set for the simulation model with an aim to accelerate a body of mass 50 kg from rest to attain a velocity of 50 m/s while traveling a distance of 3 meters. With the above objective, the required values of F_{max} for different

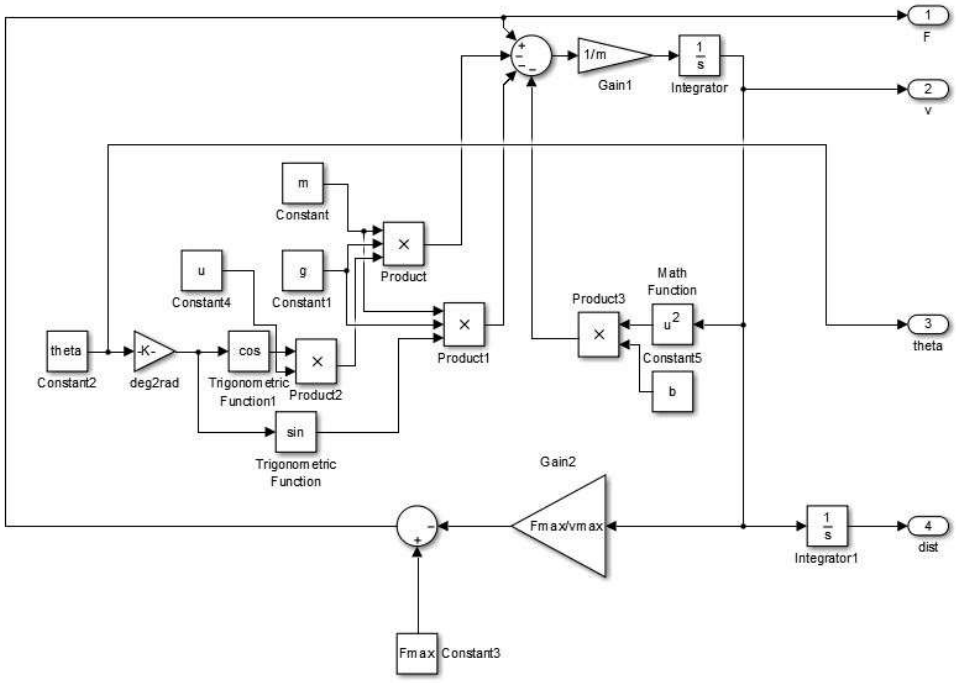

Fig. 3.3 Simulation model used for predicting SLIM performance ideal case

values of θ were found which would satisfy the performance requirements. Fig. 3.4 shows

Table 3.1 MATLAB Simulink model parameters

Parameter	Symbol	Value	Unit
Total mass of body	m	50	kg
Acceleration due to gravity	g	9.81	m/s^2
Launch angle	θ	0 - 90	degrees
Coefficient of drag force	b	0.06	N/m^2/s^2
Coefficient of kinetic friction	μ	0.35	-
Maximum velocity	v_{max}	75	m/s

that horizontal propulsion of the projectile would require the least but still a considerable amount of starting force of around 41.35 kN. Also, the starting force value does not vary much (about 1.33% as compared to horizontal propulsion case) when the propulsion angle is varied. It means that the force-velocity characteristics and hence the LIM design would remain more or less the same for any propulsion angle between 0^o and 90^o .The time to achieve the desired exit velocity can also be found, which would be crucial in deciding the

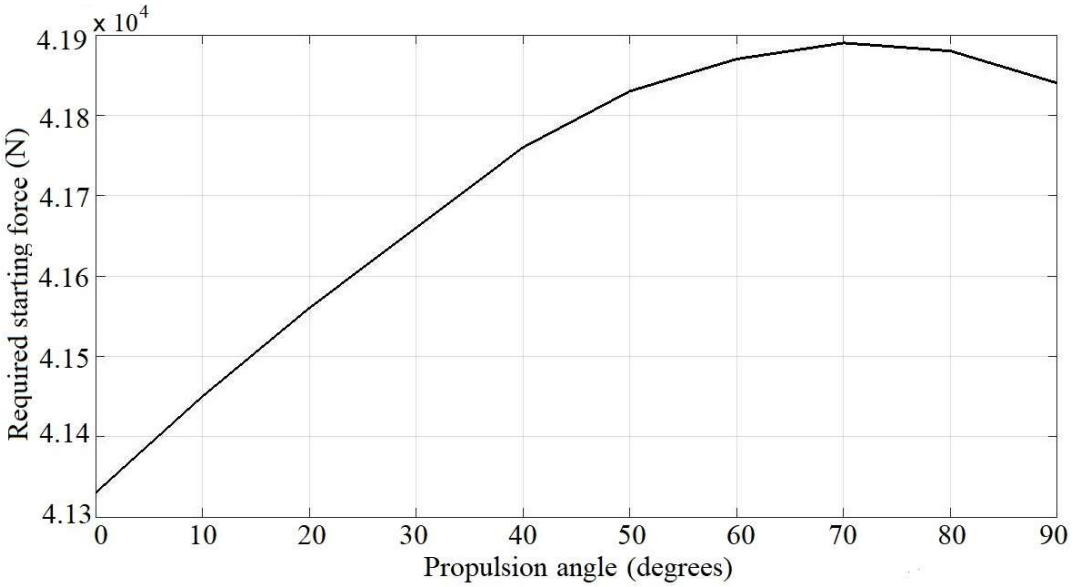

Fig. 3.4 Required values of starting force for different values of propulsion angle

operating time of the LIM and its temperature rise. Also, the power and energy required at the time of propulsion can be determined by using the force, velocity and time sample values. The results are shown for a propulsion angle of 30^o, with the rest of the parameters as indicated in Table 3.1.

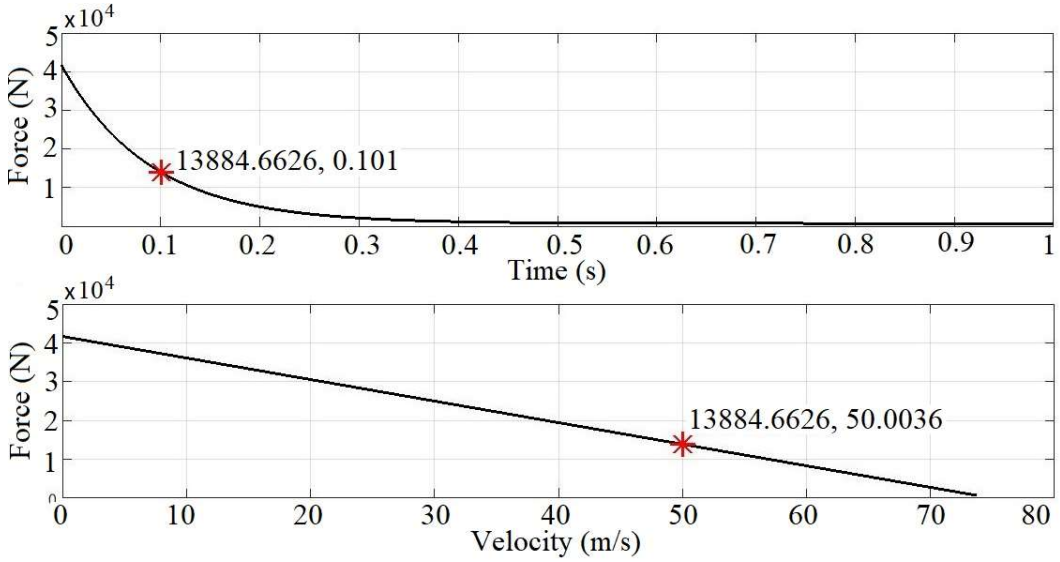

(a) Force versus time and velocity

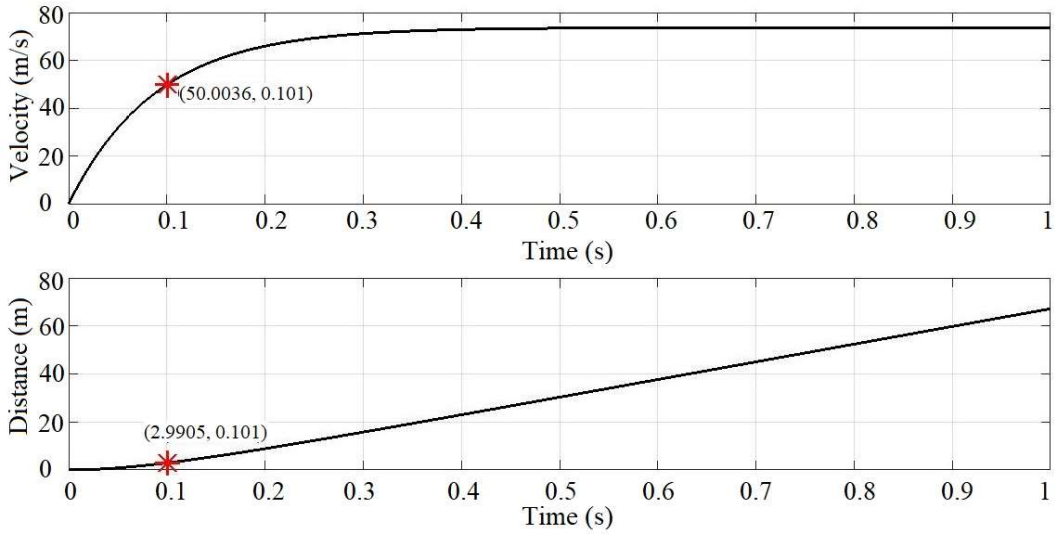

(b) Velocity and distance versus time

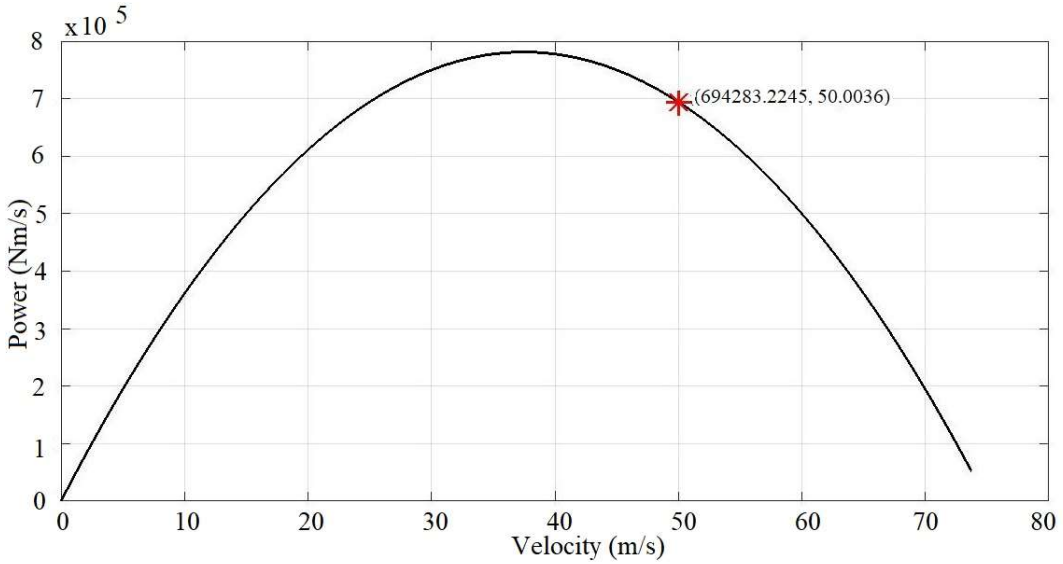

(c) Power versus velocity

Fig. 3.5a shows the force-time and the inverse linear force-velocity characteristic. With a starting force of around 42 kN, it takes 0.101 seconds for the projectile to reach the exit velocity of 50 m/s within the stipulated travel distance of 3 meters. The synchronous or maximum velocity of the LIM is chosen as 75 m/s, but the projectile will exit the EMPS when it attains a velocity of 50 m/s (Fig. 3.5b). Figs. 3.5c and 3.5d show the predicted

values of energy and power to be around 70 kJ and 694 kW respectively at the time of projectile exit.

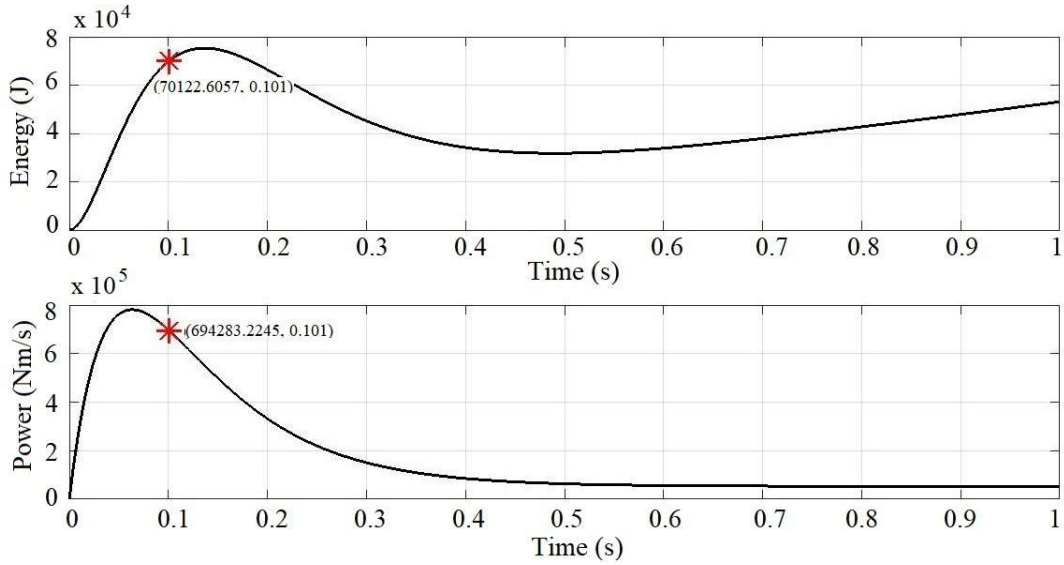

(d) Energy and power versus time

Fig. 3.5 Plots for a propulsion angle of 30^o. The red asterisk represents the instant when the projectile exits the propeller.

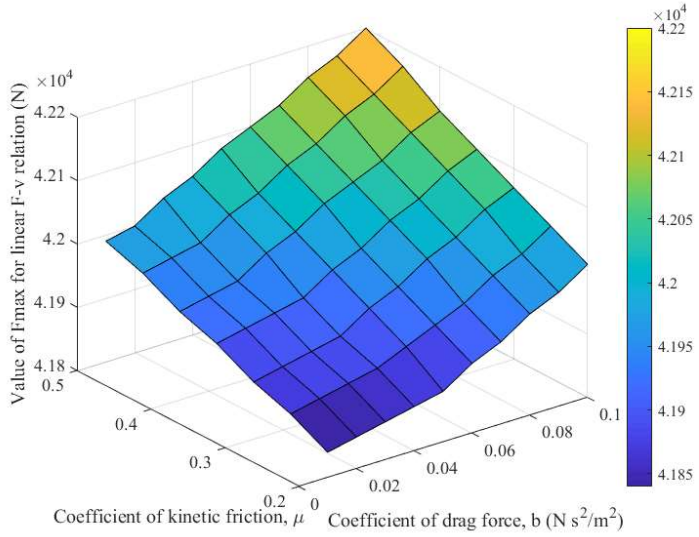

Fig. 3.6 Surface plot of the values of the starting force F_{max} for different values of coefficient of kinetic friction μ and coefficient of drag force b

Another study was done on the effect of variation of the parameters μ and b on the required value of the starting force F_{max}. As is observed from Fig. 3.6, the value of F_{max} does not vary significantly when the two coefficients are varied over their typical range of values.

3.3 Design of the LIM

The next step is to design an LIM with a similar characteristic as required in Fig.3.5a. Parseval's method was used to determine the force-velocity characteristics of a single-sided LIM (SLIM). It is to be noted that the length of the stator of SLIM must be equal to the distance traveled by the projectile i.e. 3 meters

Table 3.2 Design details of the SLIM

Parameter	Value
Primary iron core length	3000 mm
Primary iron core width	1000 mm
Secondary aluminium sheet width	3000 mm
Secondary back iron width	1000 mm
Air gap	10 mm
Secondary aluminium sheet thickness	3 mm
Secondary back iron thickness	6 mm
Slot width	25 mm
Tooth width	25 mm
Slot depth	25 mm
Number of slots	180
Conductors per slot	20
Current 70 A (rms),	99 A (peak)
Current density	1.1879×10^5 A/m
Number of poles	4
Power supply frequency	50 Hz
Stator winding arrangement	R,-B,Y, lap winding, double layer

3.3.1 Optimizing the Design Parameters

It is well known that by increasing the secondary resistance of an induction motor, linear or rotary type, its torque or force-velocity curve becomes more and more inverse linear in shape. In order to understand the effect of varying the design parameters on the performance characteristics of the SLIM, its parametric calculation has been conducted based on Parseval's method [Appendix A]. The nominal values of the parameters, i.e the values which are kept fixed while varying a parameter, unless stated otherwise, are shown in Table 3.2.

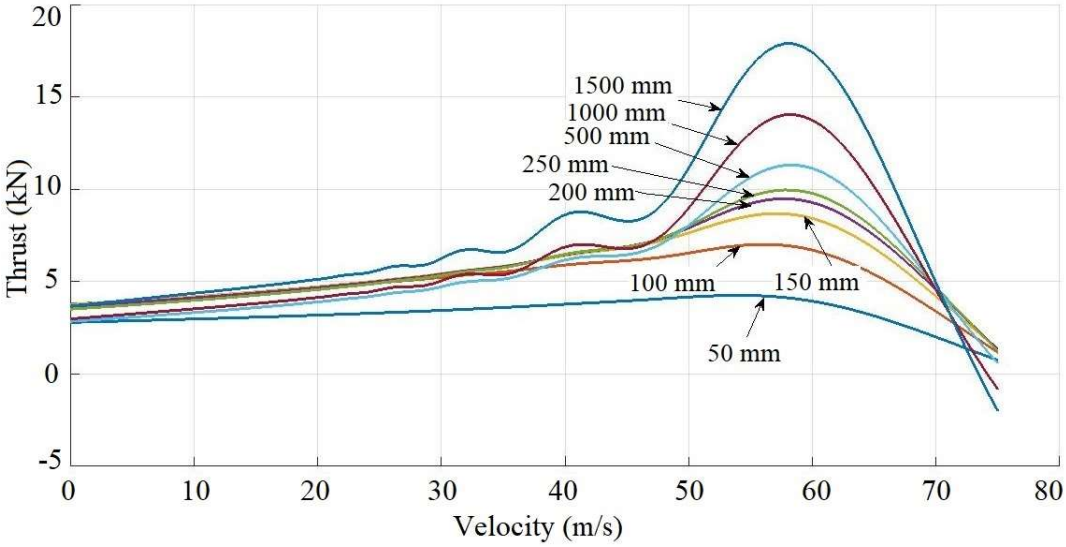

(a) Different primary iron widths

From the calculation results obtained for constant-current drive, Fig. 3.7 demonstrates the manner in which thrust alters upon varying a parameter. By increasing primary iron width (Fig. 3.7a), marked rise in the peak thrust can be seen. Here, the secondary conductor width is taken to be the double of primary iron width in the parametric study. It can be inferred that while decreasing the primary iron width may make the characteristic's shape more suitable for the considered application (closer to inverse-linear in shape), the thrust value would also abate. It is to be noted that the ratio of secondary and primary width

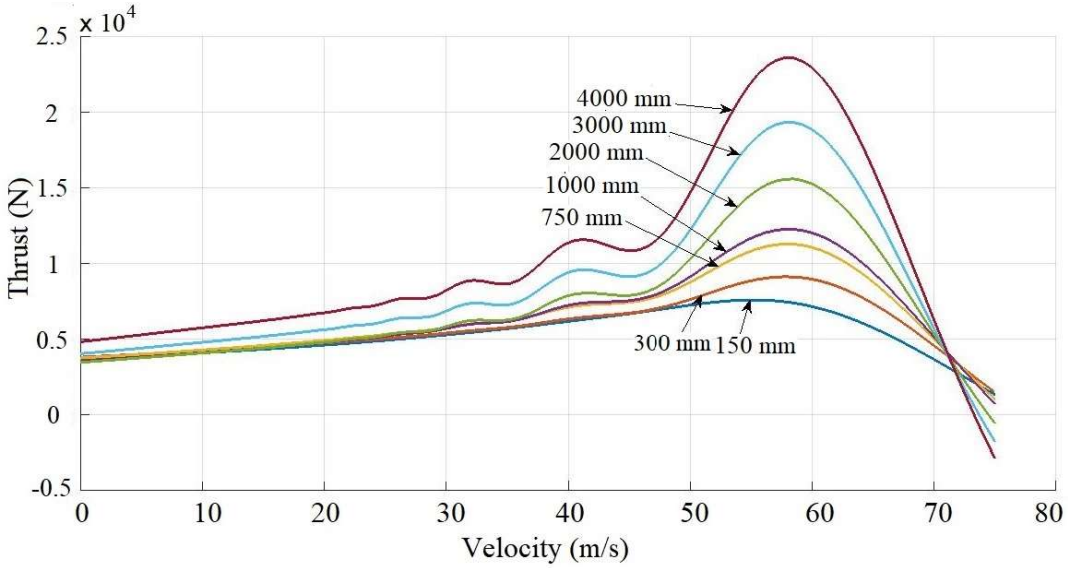

(b) Different secondary conductor widths

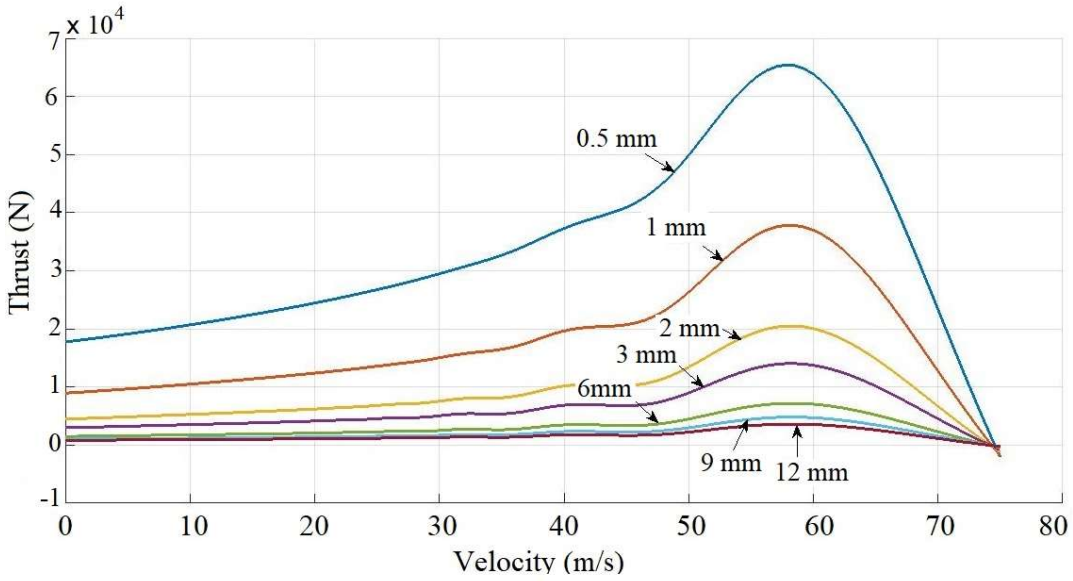

(c) Different secondary conductive sheet thicknesses

is kept fixed to be 2. Fig. 3.7b pertains to different secondary conductor widths and again the ratio of secondary and primary width is kept fixed to be 2. The peak thrust increases almost uniformly with the increasing secondary conductor width, while the starting thrust remains very much invariable like in (Fig. 3.7a). Fig. 3.7a and Fig. 3.7b

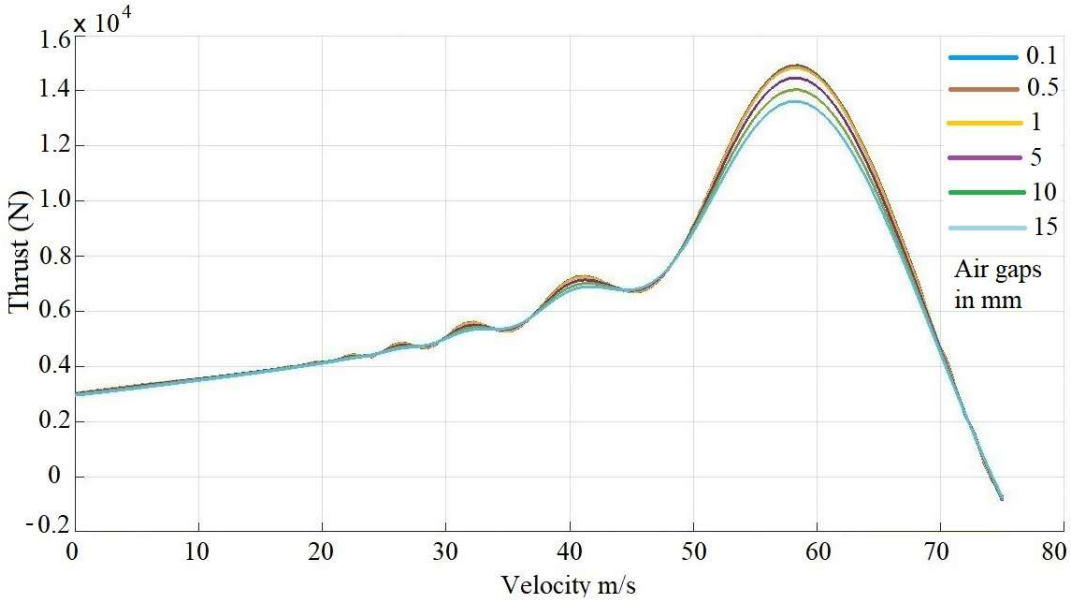

(d) Different air gaps

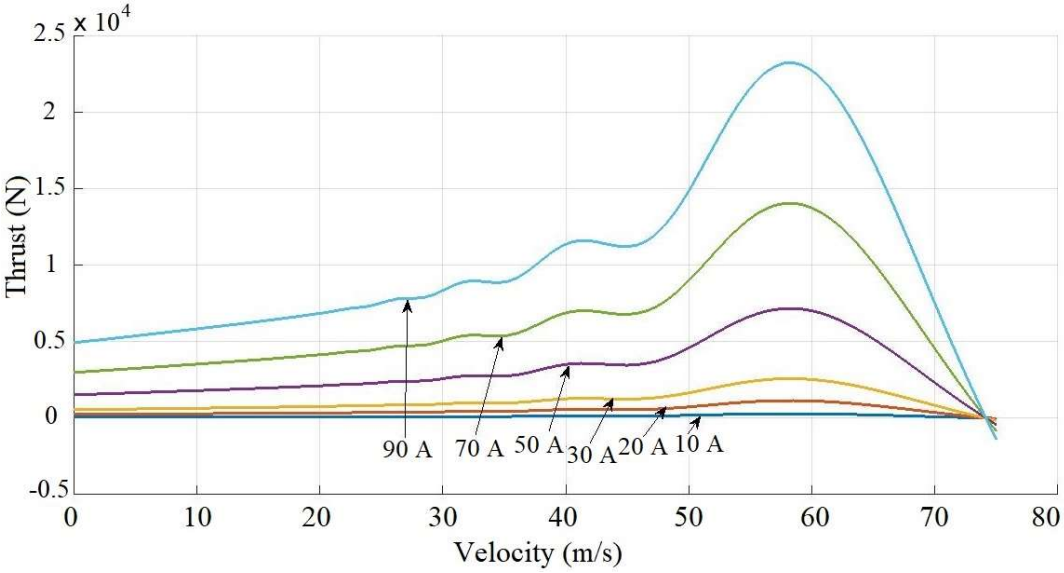

(e) Different currents

differ on account of the Russel-Norsworthy correction factor for secondary conducting sheet resistivity being incorporated in case of the latter. The rotor resistivity increases upon decreasing the secondary conductor width. This implies higher secondary resistance, which explains the characteristics to become closer to inverse-linear in shape for smaller

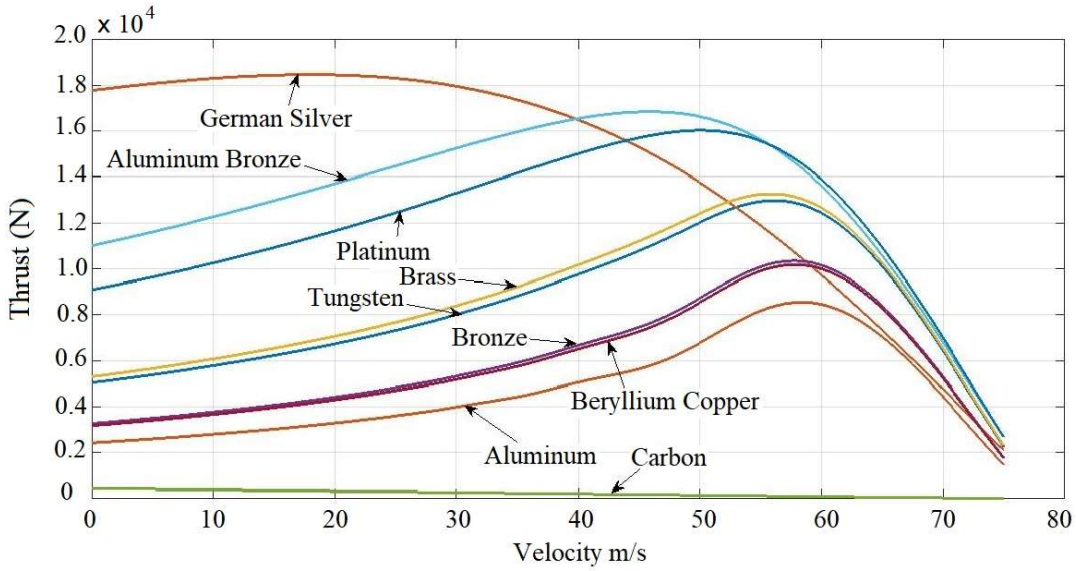

(f) Different secondary conductivities

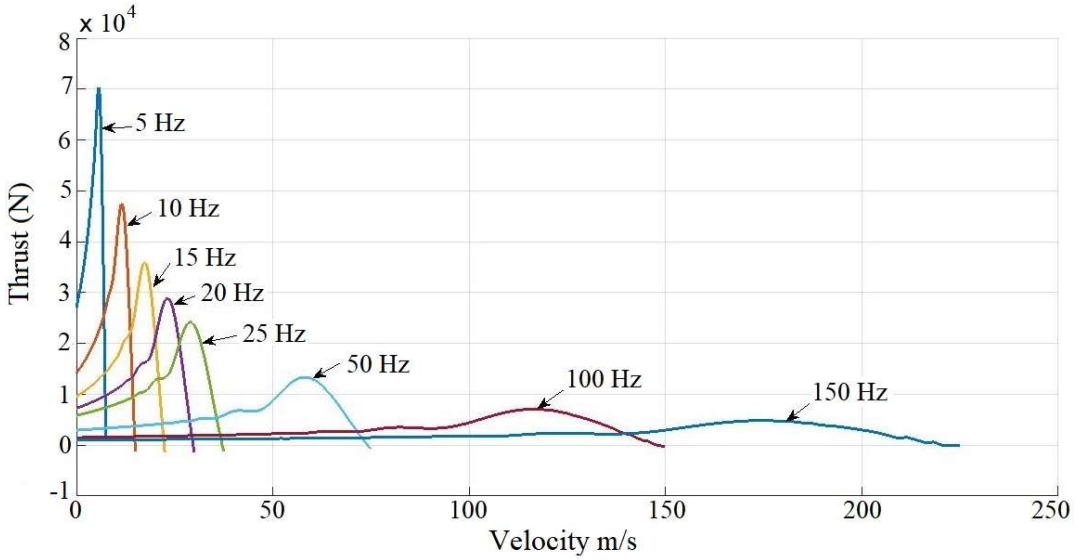

(g) Different supply frequencies

secondary conductor widths. Notwithstanding the above, it may be remembered that in the case of constant voltage drive, the smaller width of primary will result in higher input current and hence larger thrust. Furthermore, thrust multiplies with current square rule Fig. 3.7e, nonetheless, magnetic saturation will result in slight decrease in the thrust. Fig. 3.7h exhibits the behavior of the curves for different number of poles. Larger number of

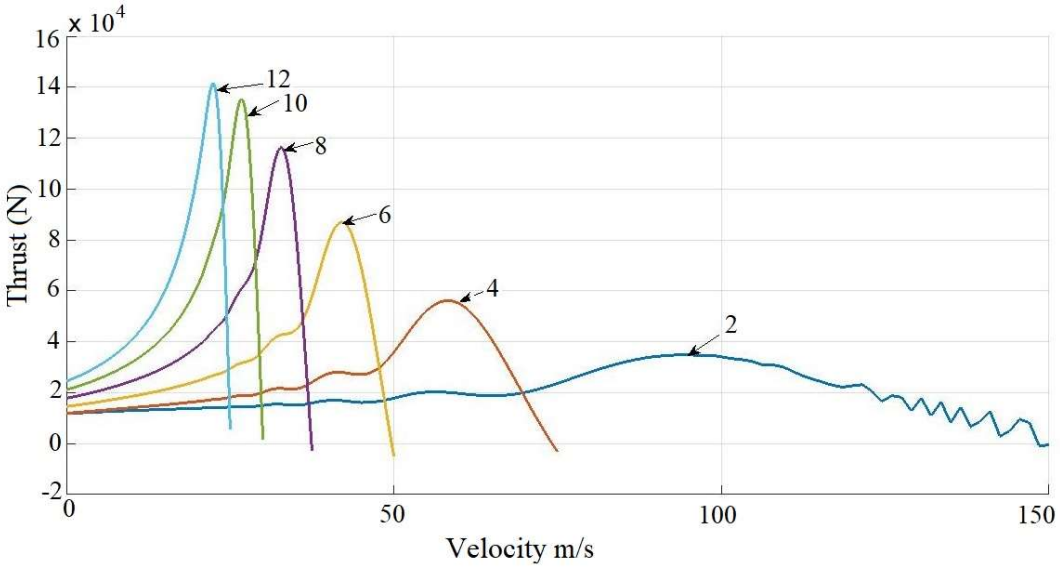

(h) Different number of poles

Fig. 3.7 Performance characteristics of SLIM with varying design parameters.

poles lead to greater thrust generated owing to the reduced pole pitches and thereby the synchronous velocities, for thrust falls off with increasing speed as the longitudinal (entry and exit end) effects become significant [53]. The thrust can also be made to surge by decreasing the air gap (Fig. 3.7d) (albeit the increase in thrust is slight when the air gap is reduced from 15 mm to 0.1 mm), supply frequency (Fig. 3.7g) (on account of the decrease in synchronous velocities) [54] and secondary conductive sheet thickness (Fig. 3.7c) (by the virtue of the reduced electromagnetic gap between the primary and the secondary iron). However, a thin layer of secondary sheet may even melt and evaporate when large eddy currents will flow. As such a suitable thickness is to be selected.

Fig.3.7f needs special inspection. Here, different metals have been evaluated for secondary sheet of conductivities in the order of 10^6 - 10^7 S/m, with the highest conductivity of aluminum at $3.77 \times 10^7 S/m$ and the lowest being that of German Silver at $3.33 \times 10^6 S/m$. Within this range thrust increases with the lowering of the conductivity. Further lessening under this range would ensue a downturn in thrust as is indicated by the

curve for carbon with conductivity of $2.88 \times 10^4 S/m$. It seems that German Silver is the most suitable candidate for electromagnetic launch with slight higher melting point of that of aluminium

The width of the secondary was decided on the basis of Russell-Norsworthy correction factor for secondary overhang for sheet rotor machines. The Russell and Norsworthy formula [55] gives a correction factor for the effective secondary surface resistivity ρ_r' as

$$\rho_r' = \rho_r/(1-k) \tag{3.7}$$

where $k = \tanh\varepsilon/[\varepsilon(1+\tanh\varepsilon\cdot\tanh\phi)]$, in which $\varepsilon = \pi w/\tau$, $\phi = \pi\psi/\tau$, w is half of the stator width, τ is the pole pitch and ψ is the width of the overhang of the rotor plate beyond the edge of the stator. Fig. 3.8 shows the secondary surface resistivity versus secondary

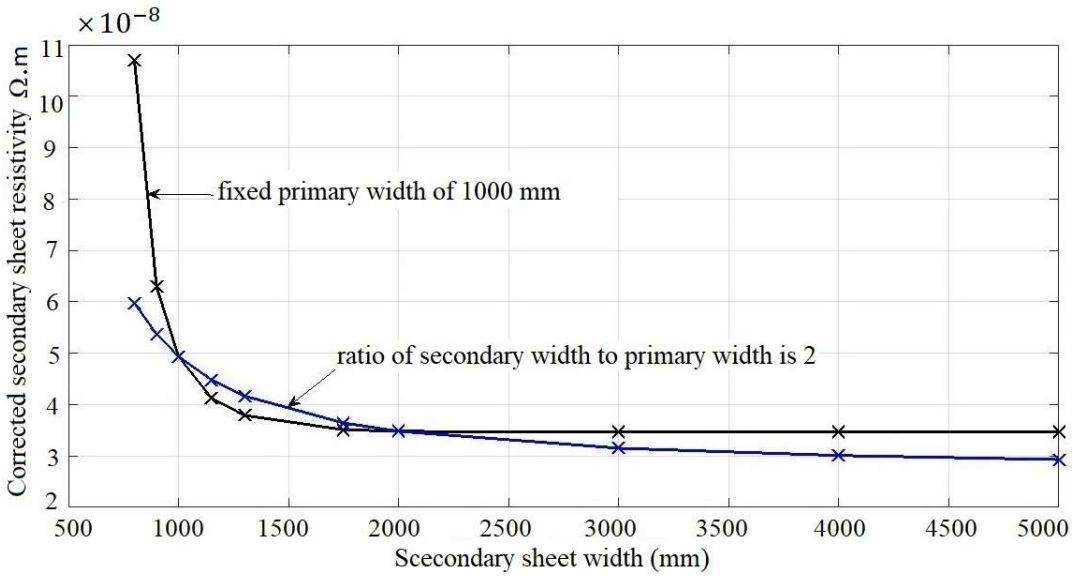

Fig. 3.8 Effective resistivity variation due to secondary overhangs

conductor width plots for fixed and variable primary iron widths. From the curves, it is observed that the rotor resistivity increases upon decreasing the secondary conductor width.

The width of the secondary should be at least twice the width of the primary for it also decreases the transverse edge effect [56].

3.3.2 Experimental Results for Thrust

Table 3.3 Parameters of the fabricated SLIM

Parameter	Value
Primary iron core length (L, mm)	560
Secondary sheet length (L_s, mm)	750
Primary iron core width ($2w$, mm)	85
Secondary sheet width ($2d$, mm)	300
Secondary back iron width ($2d_i$, mm)	145
Air gap ($a-b$, mm)	2.2
Secondary sheet thickness ($b-c$, mm)	3
Secondary back iron thickness (c, mm)	4
Number of slots	24
Number of coils (Distributed 2 layer winding)	30
Number of coil sides per slot	2
Number of turns per coil	50
Coil pitch in terms of no. of slots	6
Pole pitch (τ, mm)	140
Number of poles	4
Power supply frequency (Hz)	50
Primary Current (A) rms	15

The fabricated test rig of single sided linear induction motor (SLIM) is shown in Fig. 3.9. The design details are being given in Table 3.3. A prototype SLIM of smaller size than the proposed SLIM was fabricated and tested for different secondary conducting sheet materials to validate the performance characteristics of SLIM (Fig. 3.7f) which is one of our conclusive suggestion in the proposed work. Fig. 3.10 shows the VFD inverter, DSO for ascertaining the current, the stator and the three sheet secondary plates placed in a staggered manner above the stator. The sheet on the top is of aluminum with the back-iron glued above it, below of which is the sheet of German silver and the bottom sheet is of Beryllium copper. The fabricated LIMs have been theoretically analyzed using Fourier

Fig. 3.9 Prototype SLIM stator with sliding support for secondary sheet

Fig. 3.10 Setup for testing of the prototype SLIM

transform method (Parseval's) [5] pertaining to an equivalent SLIM. The Maxwell FEM software has been used to simulate and compute fields and forces. For standstill tests, variable frequency were obtained through 18.5 KW three phase ABB VFD. For linear induction motor, the Force-speed characteristics and Standstill Force versus slip frequency characteristics are quite identical with certain tolerance because of the absence of end effects in standstill condition.

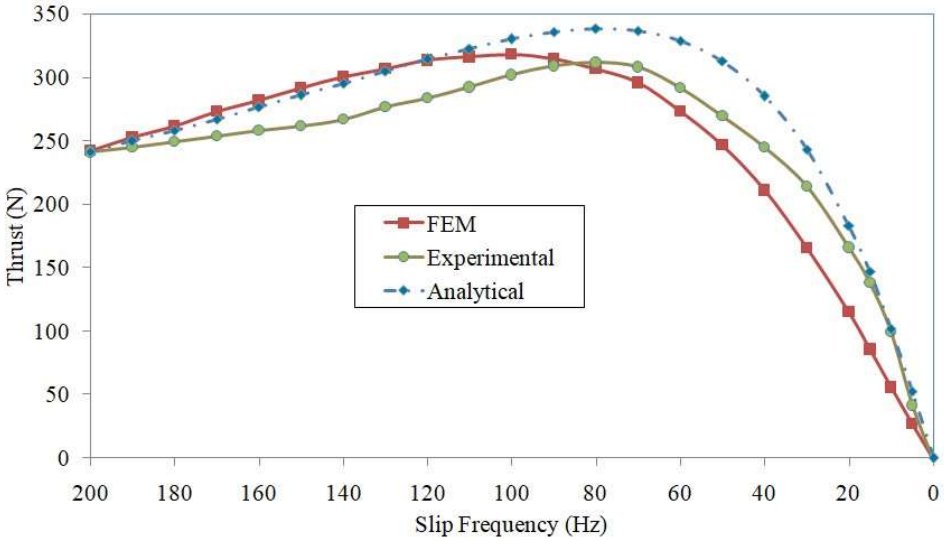

Fig. 3.11 Thrust for SLIM with Aluminum as the secondary

While Fig. 3.11 depicts the constant current (15A) normalized values measured and computed force of developed SLIM at different slip frequencies for aluminum as the secondary, Fig. 3.12 pertains to German Silver and Fig. 3.13 to Beryllium copper (conductivity of $2.865 \times 10^6 S/m$). The characteristics of aluminum and beryllium copper are quite identical. All the above three materials were of non-magnetic grade. The Finite Element and analytically computed forces are on the higher side due to the assumptions made and also because of slightly unbalanced three phase supply obtained during experimentation. It can be inferred that German Silver gives better thrust characteristics than aluminum as the secondary sheet material.

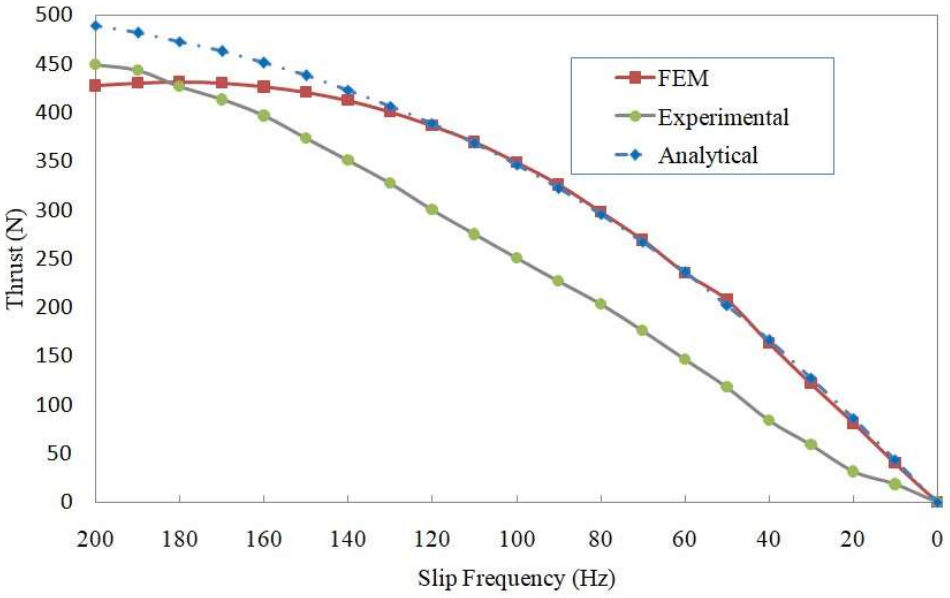

Fig. 3.12 Thrust for SLIM with German Silver as the secondary

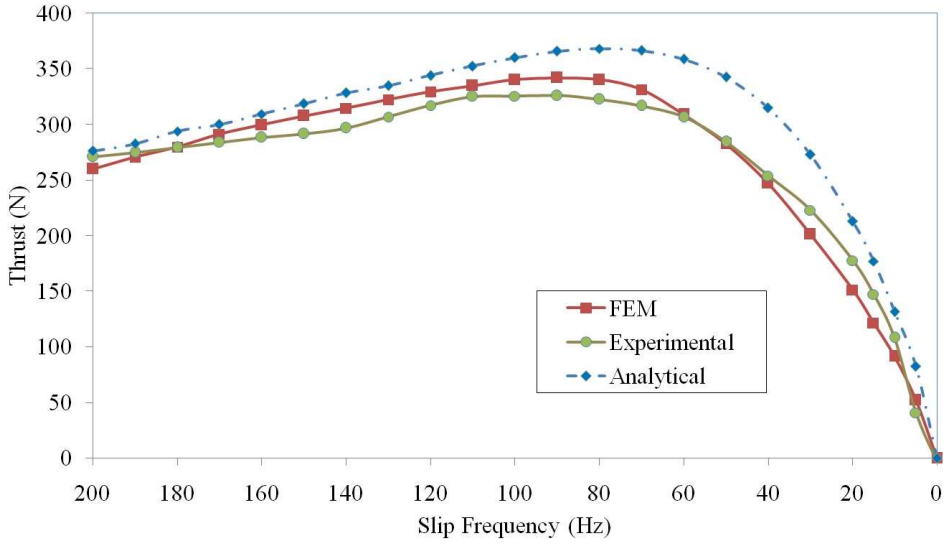

Fig. 3.13 Thrust for SLIM with Beryllium copper as the secondary

3.3.3 SLIM DESIGN

The design parameters of the SLIM are chosen based on the study of parameter variation done and which are shown in Table 3.2. The above design of the SLIM is analyzed using

Parseval's method and its performance characteristics are obtained (Figs. 3.14a and 3.14b). The force-velocity characteristic obtained in Fig. 3.14a needs to be amplified by a factor of about 4 in order to satisfy the conditions of the 3 m distance travel and 50 m/s exit velocity.

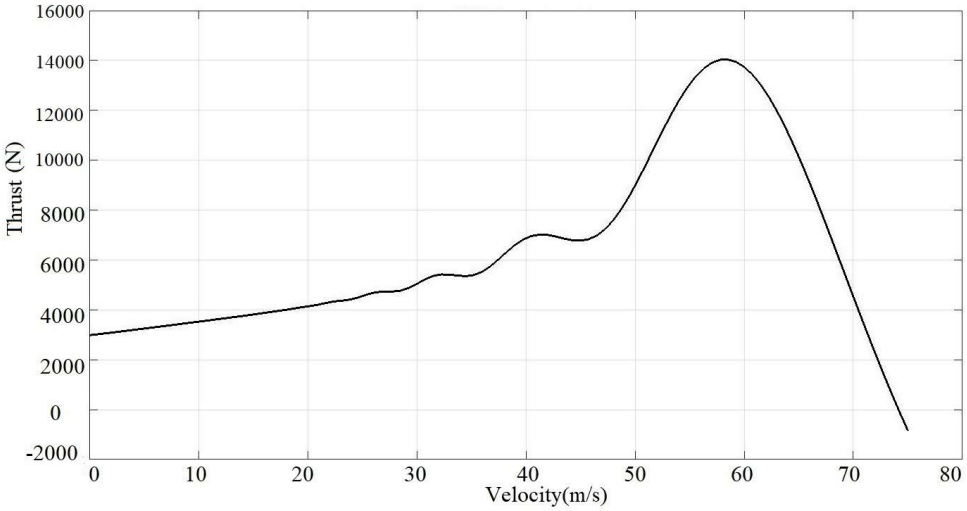

(a) Thrust-velocity characteristic

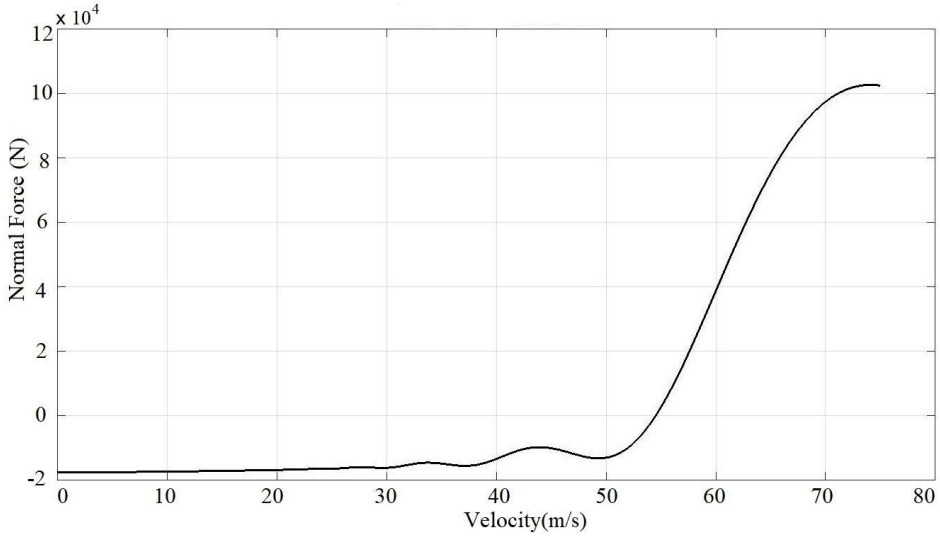

(b) Normal force versus velocity curve

Fig. 3.14 Performance characteristics of the designed SLIM. Gain required = 3.974.

This can be done by doubling the conductors per slot, as force is proportional to current density squared. The performance of the then designed SLIM for propulsion application

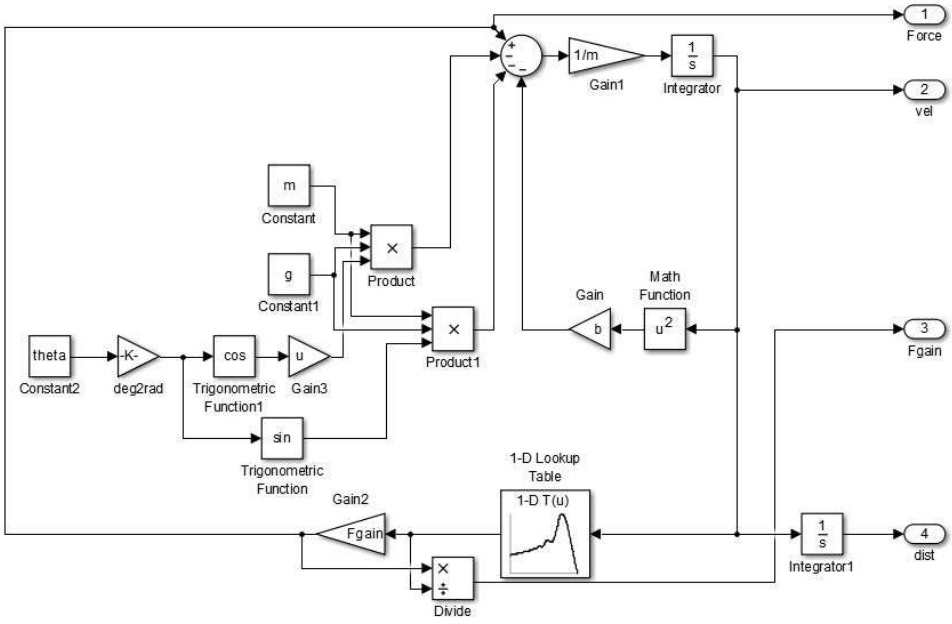

Fig. 3.15 Simulation model used for predicting SLIM performance while operating

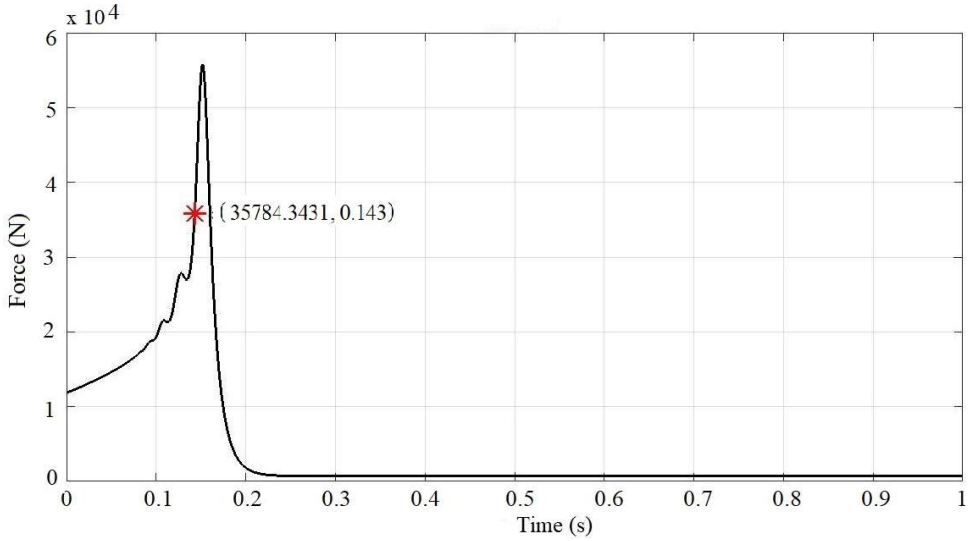

Fig. 3.16 Force versus time curve

was predicted by using the developed Simulink Model. In place of the inverse-linear relation between force and velocity, the actual characteristics of the designed SLIM are used for establishing the relation between force and velocity. The modified MATLAB Simulink model is depicted in Fig.3.15.

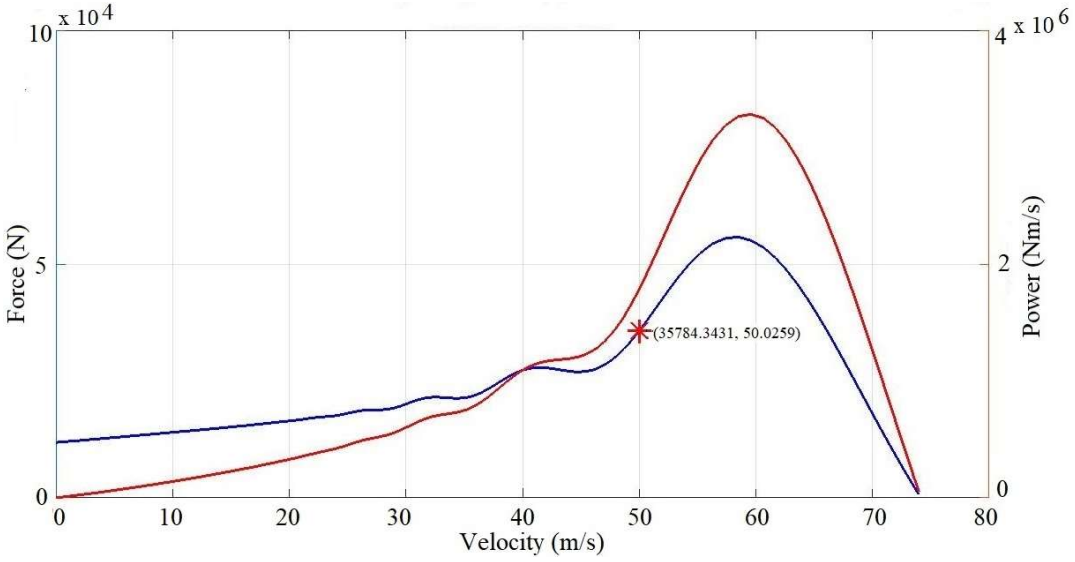

Fig. 3.17 Force and power versus velocity curves

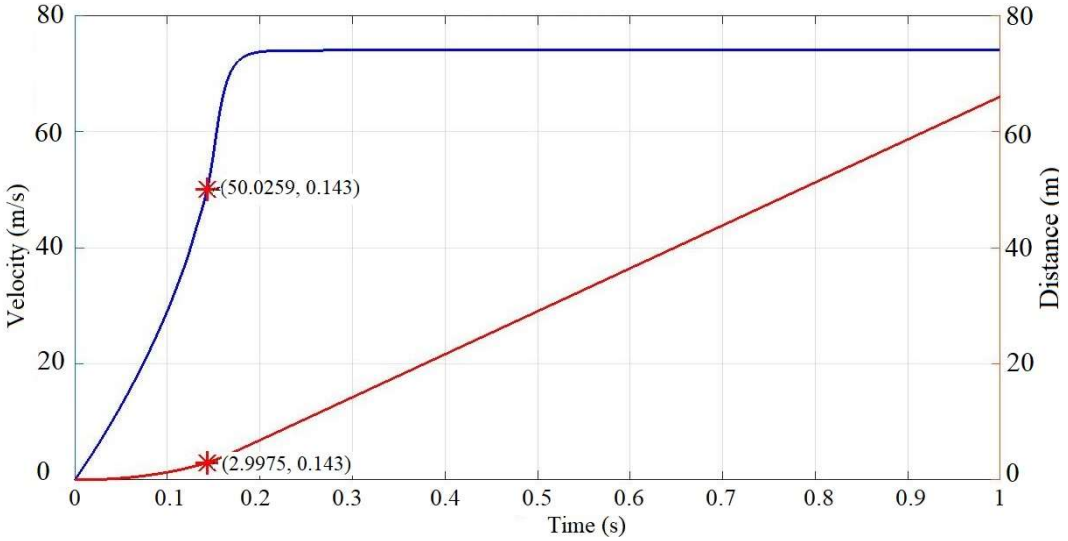

Fig. 3.18 Velocity and distance versus time curves

Figs. 3.16, 3.17, 3.18 and 3.19 show the predicted performance of the designed SLIM-assisted EMPS, which seems to be poorer than that observed for the ideal case (Fig. 3.5). The projectile takes about 0.143 seconds to reach the velocity of 50 m/s and travel 3 metres. The energy and power values at the time of exiting the propeller are around 256 kJ and 1.7 MW respectively, both of which are considerably higher than the values obtained for the

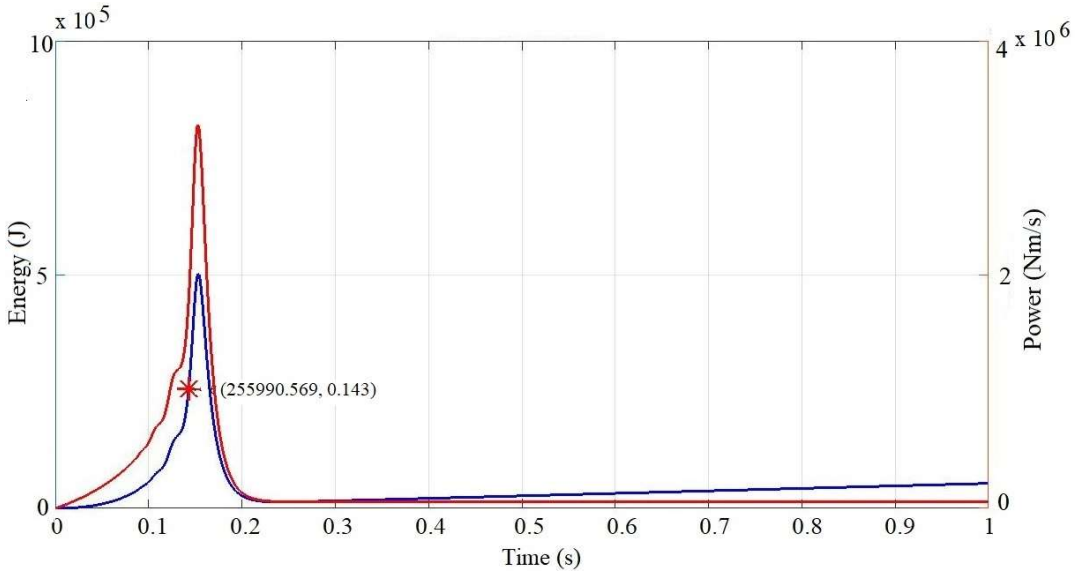

Fig. 3.19 Energy and power versus time curves

ideal case. This goes on to show how the design of the SLIM would affect its propulsion performance and power supply and cooling requirements.

3.4 Conclusion

The present Chapter has dealt with the constant current studies of SLIM for EM launch. The parametric studies reported have been computed using Parseval's Transform. The effect of conducting secondary plate material has been determined and it has been found that German Silver is the most suitable material for EM launch. Using one prototype SLIM analytical, FEM and test results at standstill condition for variable frequencies and at materials- Aluminum, Beryllium Copper and German Silver has been reported. The next Chapter deals with a more realistic method of constant voltage analysis for different types of windings.

****